

Syntheses and Characterization of Well-Crystallized Birnessite

D. S. Yang and M. K. Wang*

Department of Agricultural Chemistry, National Taiwan University, Taipei, Taiwan

Received January 4, 2001. Revised Manuscript Received June 5, 2001

A modified oxidation–deprotonation reaction (ODPR) was developed to synthesize well-crystallized birnessite. We compared the conventional methods for synthesis of birnessite with the ODPR approach. The structural chemistry of birnessite was evaluated by high-resolution transmission electron microscopy (HRTEM), using an energy-dispersive spectrometer (EDS) to determine the Na⁺ content. The average oxidation states (AOS) of birnessite were determined by potentiometric titration. Infrared spectrometric (IR) and X-ray diffraction (XRD) analytical techniques were used to characterize birnessite. The HRTEM lattice image and low Na⁺ content suggest that there are no vacancies in the octahedral layers of birnessite. The AOS values of birnessite ranged from 3.77 to 3.87 and the presence of IR bands at 1153 and 1084 cm⁻¹ were attributed to the Mn³⁺–OH deformation. The results show evidence for the presence of the Mn³⁺ or Mn²⁺ in the structure of birnessite.

Introduction

Birnessite has been found in ores,^{1,2} soils,^{3–6} or manganese nodules on the sea floor.^{5,7–9} Birnessite was first identified by Jones and Milne (1956)¹⁰ at Aberdeenshire in Scotland. This mineral is characterized by a platy structure with a corresponding X-ray diffraction peak around 0.7 nm.¹⁰ Birnessite has been well-known for its high specific area and low point zero charge (PZC). Therefore, it can be used as a scavenger for heavy metals.^{11–15} Birnessite also possesses catalytic properties which play an important role in the genetic process of humic substances in soils.^{16–18} However, some earlier reports indicated that birnessite is not only a potential catalytic material^{19–21} but also an important precursor

as an octahedral molecular sieve (OMS).^{22–34} Mn⁴⁺–oxides have received a lot of attention because of their high potential to be used as OMS. For example, todorokite with a 3 × 3 MnO₆ tunnel framework has been investigated for its potential catalytic power.^{27,31} Thus, the relationship between birnessite and OMS products has aroused much interest. Improved methods for crystallizing birnessite may result in production of high-quality OMS.^{26,27}

During the 1980s, several researchers followed Giovanoli's method^{22,23} of oxidizing pyrochroite with oxygen in NaOH solution (designated as the OPO method) to prepare birnessite.^{19,24,25,35–39} However, hausmannite can be easily formed with irreproducible products when the conventional OPO method is used. Some alternative

* To whom correspondence should be addressed. Tel.: (0118862) 2363-0231, ext. 2491 or 3066. Fax: (0118862) 2366-0751. E-mail: mkwang@ccms.ntu.edu.tw.

- (1) DeVilliers, J. E. *Econ. Geol.* **1983**, *78*, 1108.
- (2) Usai, A.; Mita, N. *Clays Clay Miner.* **1995**, *43*, 116.
- (3) Potter, R. M.; Rossman, G. R. *Am. Miner.* **1979**, *64*, 1199.
- (4) McKenzie, R. M. *Pac. Sci.* **1983**, *37*, 85.
- (5) Uzoichukwu, G. A.; Dixon, J. B. *Soil Sci. Soc. Am. J.* **1986**, *50*, 1358.
- (6) Golden, D. C.; Dixon, J. B.; Kanehiro, Y. *Aust. J. Soil Res.* **1993**, *31*, 51.
- (7) Lonsdale, P.; Burn, V. M.; Fisk, M. *J. Geol.* **1980**, *88*, 611.
- (8) Alpin, A.; Cronan, D. S. *Geochim. Cosmochim. Acta* **1985**, *49*, 437.
- (9) Varentsov, I. M.; Drits, V. A.; Gorshkov, A. I.; Sivtsov, A. V.; Sakharov, B. A. *1991 Mar. Geol.* **1991**, *96*, 53.
- (10) Jones, L. H.; Milnes, A. A. *Mineral. Magn.* **1956**, *31*, 283.
- (11) Giovanoli, R. *Chimica* **1975**, *29*, 517.
- (12) McKenzie, R. M. *Aust. J. Soil Res.* **1980**, *18*, 61.
- (13) Dillard, J. G.; Crowther, D. L.; Murray, J. W. *Geochim. Cosmochim. Acta* **1982**, *46*, 755.
- (14) Hein, J. R.; Schwab, W. C.; Davis, A. *Mar. Geol.* **1988**, *78*, 255.
- (15) Cowen, J. P.; Massoth, G. J.; Feely, R. A. *Deep-Sea Res.* **1990**, *37*, 1619.
- (16) Shindo, H.; Huang, P. M. *Nature* **1982**, *298*, 363.
- (17) Shindo, H.; Huang, P. M. *Soil Sci. Soc. Am. J.* **1984**, *48*, 927.
- (18) Wang, M. C.; Lin, C. H. *Soil Sci. Soc. Am. J.* **1993**, *57*, 88.
- (19) Golden, D. C.; Dixon, J. B.; Chen, C. C. *Clays Clay Miner.* **1986**, *34*, 511.
- (20) Segal, S. R.; Park, S. H.; Suib, S. L. *Chem. Mater.* **1977**, *9*, 98.
- (21) Luo, J.; Huang, A.; Park, S.; Suib, S. L.; O'Young, C. L. *Chem. Mater.* **1998**, *10*, 1561.

- (22) Giovanoli, R.; Stahli, E.; Feitknecht, W. *Helv. Chim. Acta* **1970**, *53*, 209.
- (23) Giovanoli, R.; Stahli, E.; Feitknecht, W. *Helv. Chim. Acta* **1970**, *53*, 453.
- (24) Chen, C. C.; Golden, D. C.; Dixon, J. B. *Clays Clay Miner.* **1986**, *34*, 565.
- (25) Golden, D. C.; Dixon, J. B.; Chen, C. C. *Clays Clay Miner.* **1986**, *34*, 511.
- (26) Post, J. E.; Bish, D. L. *Am. Miner.* **1988**, *73*, 861.
- (27) Wong, S. T.; Cheng, S. *Inorg. Chem.* **1992**, *31*, 1165.
- (28) Shen, Y.-F.; Zenger, R. P.; DeGuzman, R. N.; Suib, S. L.; McCurdy, L.; Potter, D. I.; O'Young, C. L. *J. Chem. Soc. Chem. Commun.* **1992**, *17*, 1213.
- (29) Shen, Y.-F.; Zenger, R. P.; DeGuzman, R. N.; Suib, S. L.; McCurdy, L.; Potter, D.; O'Young, C. L. *Science* **1993**, *260*, 511.
- (30) DeGuzman, R. N.; Shen, Y.-F.; Shaw, B. R.; Suib, S. L.; O'Young, C.-L. *Chem. Mater.* **1993**, *5*, 1395.
- (31) DeGuzman, R. N.; Shen, Y.-F.; Neth, E. J.; Suib, S. L.; O'Young, C.-L.; Levine, S.; Newsam, J. M. *Chem. Mater.* **1994**, *6*, 815.
- (32) Yin, Y.-G.; Xu, W.-Q.; Shen, Y.-F.; Suib, S. L. *Chem. Mater.* **1994**, *6*, 1803.
- (33) Yin, Y.-G.; Xu, W.-Q.; DeGuzman, R.; Suib, S. L. *Inorg. Chem.* **1994**, *33*, 4384.
- (34) Tian, Z.-R.; Yin, Y.-G.; Suib, S. L.; O'Young, C. L. *Chem. Mater.* **1997**, *9*, 1126.
- (35) Paterson, E. *Am. Miner.* **1981**, *66*, 424.
- (36) Paterson, E.; Bunch, J. B.; Clark, D. R. *Clay Miner.* **1986**, *21*, 949.
- (37) Cornell, R. M.; Giovanoli, R. *Clays Clay Miner.* **1988**, *36*, 249.
- (38) Kung, K. H.; McBride, M. B. *Clays Clay Miner.* **1988**, *36*, 297.
- (39) Post, J. E.; Veblen, D. R. *Am. Miner.* **1990**, *75*, 477.

methods have thus been developed to replace the conventional OPO approach. One of them is to prepare birnessite by oxidizing pyrochroite with permanganate (designated as the OPP method) instead of oxygen.^{21,40–44} Although the OPP method has the advantage of producing high-quality birnessite, it is time-consuming.

This study attempted to improve the conventional OPO method and prepare well-crystallized birnessite without any impurities using the modified oxygen–deprotonation reaction (ODPR) method. To prepare pyrochroite without the presence of Mn³⁺, both NaOH and Mn²⁺ solutions must be purged with nitrogen gas before they are mixed with each other to exclude oxygen from these solutions. Pyrochroite suspensions are oxidized at different concentrations of NaOH and oxygen to form birnessite or randomly stacked birnessite. This study also compared the ODPR approach with the conventional OPO and OPP methods and assessed the structural chemistry of the well-crystallized birnessite. The analytical tools used included X-ray diffraction (XRD), an infrared spectrometer (IR), average oxidation states (AOS) of Mn–oxides, high-resolution transmission electron microscopy (HRTEM), and energy-dispersive spectrometer (EDS) techniques.

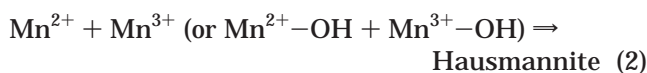
Model of the Oxidation–Deprotonation Reaction (ODPR)

To synthesize well-crystallized birnessite, the ODPR method was developed,^{45,46} as shown in the following equations:

Target reactions:



Side reactions:



Step 1: Mn²⁺ ions are oxidized quickly to Mn⁴⁺, followed by hydrolysis that converts Mn²⁺–OH to Mn⁴⁺–OH.

Step 2: Random stacked birnessite ages at high temperature and transforms into birnessite.

According to the ODPR method, whether random stacked birnessite or hausmannite is formed depends on the onset of pyrochroite oxidation, and the reaction of pyrochroite into random stacked birnessite is favored under rapid oxidization. Thus, pyrochroite oxidation was carried out under an oxygen gas flow rate at 5 L/min for the first 30 min. Thereafter, the oxygen flow rate

was reduced to 1 L/min and maintained at this rate for another 5 h.

The side reaction of hausmannite is favored by two conditions. The first is the presence of Mn³⁺ ions in the solutions before mixing with NaOH and heating the suspensions at high temperature. Formation of birnessite is influenced more by the former than the latter. Thus, the presence of Mn³⁺ in the solution inhibits the initial reaction. Following the ODPR approach, we can synthesize birnessite at higher temperature (i.e., from ambient temperature to 373 K) without any impurities.

Experimental Section

Synthesis of Birnessite. All manganese oxides were prepared using the ODPR approach modified from the conventional OPO method. The procedure began with dissolving 5.50 g of manganese chips in 50 mL of 6 M HClO₄. After all the manganese was dissolved, the solution was diluted to 250 mL with double-distilled water (DDW) and the final concentration of the Mn²⁺ solution was 0.4 M. The 0.4 M Mn²⁺ solution was then poured into a bottle held in a water bath at 273 K. The dissolved Mn²⁺ solution was mixed with 8 M NaOH (Merck, GR, max 0.0002% K). Meanwhile, the mixed solution was agitated at a speed of 200 rpm. Volumes of all pyrochroite suspensions were adjusted to 500 mL with DDW. The final concentrations of Mn²⁺ and NaOH were 0.2 and 4 M, respectively. To remove oxygen from the Mn²⁺ and NaOH solutions before they were mixed, high-purity nitrogen gas (above 99.9% purity) was purged into the solution at a nitrogen flow rate of greater than 0.5 L min^{−1} for at least 5 min. These two oxygen-free solutions were blended to form pyrochroite without Mn³⁺. The nitrogen was constantly purged into the pyrochroite suspensions at rates greater than 5 L min^{−1}.

The almost white suspension of pyrochroite was kept at 273 K in a water bath for 30 min. Then, the nitrogen gas was immediately replaced by oxygen. Oxidation of pyrochroite was achieved by purging with oxygen. The flow rate of oxygen was set at 5 L min^{−1} for 30 min and at 1 L min^{−1} for the following 5 h. During the oxidation process, pyrochroite suspensions were vigorously stirred. The mixing speed was increased to 300 rpm as soon as oxygen bubbles began to appear. Upon completion of all these steps, a black suspension with a blue tint was observed. The suspensions were aged between 313 and 373 K for 48 h. The aged products were centrifuged, with the supernatants discarded, and re-suspended with DDW. These processes were repeated five times to remove any salts. The precipitates were collected, freeze-dried, and stored for further analysis.

Synthesis of Feitknechtite (β-MnOOH) for the Infra-red Study. Manganese chips (0.55 g) were dissolved in 2 mL of HClO₄ solution (12 M) and diluted to 50 mL with DDW and titrated with an autotitrator (Mettler DL 25). Oxygen was removed from the Mn²⁺ solution by bubbling with nitrogen gas. Oxygen-free 8 M NaOH solution was used as a titrant. The pH of the Mn²⁺ solution was set at 12 by the titrant. As soon as the pH reached 12, nitrogen gas was immediately replaced by oxygen. In the first 15 min, the flow rate of oxygen was set at 5 L min^{−1} and then the rate was reduced to 0.5 L min^{−1} for another 45 min. During the reaction period, the solution pH was kept at 12 by the titrant. After the reaction was completed, the feitknechtite precipitates were the major phase.

X-ray Diffraction (XRD). To check whether birnessite was formed or not, oriented thin film samples supported on pieces of filter membrane (0.45 μm, 25 mm diameter) were scanned continuously at a rate of 2° min^{−1} with a Rigaku Miniflex X-ray diffractometer. Cu Kα radiation was used in the XRD studies of these oriented samples. To identify various species in all manganese oxides (MOs), a Philips PW 1729 X-ray diffractometer was used for powder X-ray diffraction studies using Cu Kα radiation with a step scan of 0.02° (2θ).

High-Resolution Transmission Electron Microscopy (HRTEM) and Energy-Dispersive Spectroscopy (EDS).

(40) Ching, S.; Landrigan, J. A.; Jorgensen, M. L. *Chem. Mater.* **1995**, *7*, 1064.

(41) Ching, S.; Petrovay, D. J.; Jorgensen, M. L.; Suib, S. L. *Inorg. Chem.* **1997**, *36*, 883.

(42) Luo, J.; Suib, S. L. *J. Phys. Chem. B* **1997**, *101*, 10403.

(43) Ma, Y.; Luo, J.; Suib, S. L. *Chem. Mater.* **1999**, *11*, 1972.

(44) Ressler, T.; Brock, S. L.; Wong, J.; Suib, S. L. *J. Phys. Chem. B* **1999**, *103*, 6407–6420.

(45) Yang, D. S.; Wang, M. K. *J. Chin. Agric. Chem. Soc.* **1991**, *29*, 106.

(46) Yang, D. S. Ph.D. Thesis, National Taiwan University, 1996; p 216.

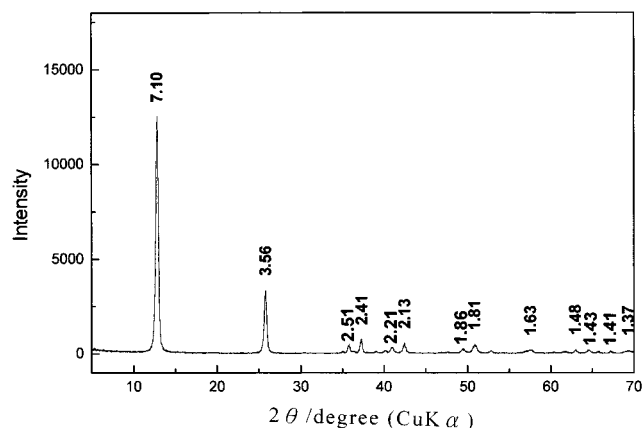


Figure 1. XRD pattern of birnessite.

A HRTEM (Hitachi FEM 2000) was used to observe lattice images of the product. The operation voltage was 200 kV. EDS was performed using a JEOL AEM 3010, equipped with Link EXL2. The results were determined at an operating voltage of 200 kV and probe size of 10 or 25 nm. Copper was used as a standard of semiquantitative analysis. After EDS analysis, the molar ratio of sodium to manganese was calculated by the equation below:

$$\text{Atomic \% of Na} / (\text{atomic \% of Na} + \text{atomic \% of Mn}) = \text{molar ratio of Na to Mn} \quad (3)$$

Average Oxidation States (AOS) of Mn. Potentiometric titration measurements were used to analyze AOS of manganese. Acidified 0.052 M oxalic acid (60 mL) was used to dissolve definite amounts of birnessite or 5-mL suspensions of MOs (in the cases of high concentration NaOH) and then diluted to 100 mL. The amount of Mn and excess oxalic acid were determined with an atomic absorption spectrophotometer (AAS) and with a previously standardized 0.03 M potassium permanganate solution. The AOS of manganese in birnessite was calculated on the basis of these two results.

Infrared Analysis (IR). All mid-IR spectra were obtained using a diffuse reflectance infrared Fourier transformation (DRIFT, Graseby Specac) accessory installed in a Bio-Rad FTS-7 IR spectrometer. Samples were scanned 512 times between 4000 and 600 cm^{-1} at a resolution of 1 cm^{-1} . The samples were prepared by blending 4 mg of the freeze-dried product (birnessite or feitknechtite) with 500 mg of oven-dried KBr (Merck, spectroscopy Uvasol) in an agate mortar. The resulting KBr mixture was packed into a holder specialized for DRIFT.

Far IR spectra from 625 to 200 cm^{-1} were collected using a Bomem MB 100 FT-IR. The sample was diluted with polyethylene powder (Merck, spectroscopy Uvasol) and the ratio of birnessite to polyethylene was 1:200. Forty milligrams of the mixture was pressed into a pellet with a diameter of 13 mm.

Results

X-ray diffractograms of synthetic birnessite showed very strong peaks at d spacings of 7.10, 3.56, 2.51, 2.41, 2.21, 2.13, 1.86, 1.81, 1.63, 1.48, 1.43, 1.41, and 1.37 Å (Figure 1) (JCPDS 23-1046). These 13 XRD peaks are a primary characteristic of birnessite^{22,23} without the presence of hausmannite (JCPDS 24-734) or feitknechtite (JCPDS 18-804). The XRD pattern is similar to that observed by Luo et al. (1998)²¹ on samples aged for 75 days. Our previous powder XRD pattern further showed that it is a well-crystallized birnessite without any impurities.⁴⁵⁻⁴⁷

Table 1. Number of Points of Birnessite Particles Analyzed by EDS

range of molar ratio ^a	N.D. ^b	0.01–0.02	0.02–0.04	0.04–0.08
number of points	11	9	3	2

^a Range of molar ratio (Na to Mn) is calculated using eq 3. ^b N.D. indicates not detected. Minimum detectable limits (MDL) of EDS is less than 1 at. %.

As seen in Figure 2, the TEM observations are in good agreement with the XRD results. Well-crystallized birnessite particles with long, platy morphology constituted the major phase and there were essentially no cubic particles of hausmannite. In general, all results of XRD and TEM analyses showed that synthetic birnessite produced by the ODPR approach resulted in high-purity and well-crystallized birnessite.

The atomic arrangement on the ab plane of birnessite was observed by HRTEM (Figure 3). The atomic arrangement of Figure 3 shows an amorphous domain at the lower left corner. Although no vacancies exist in the octahedral layer of birnessite (Figure 3), some may still remain in the amorphous domain. However, it is hard to distinguish whether these vacancies are defects or characteristic structural features of birnessite.

Figure 4 displays the results of mid-IR spectra between 3800 and 2500 cm^{-1} of birnessite. The IR spectra exhibit two sharper bands, 3450 and 3310 cm^{-1} . Luo et al.²¹ reported that these IR bands are due to interlayer hydrates and, possibly, some hydroxyl groups not from hydrates but those directly bound to the interlayer metal ions. The spectra between 1300 and 1000 cm^{-1} (Figure 5) were different from those of earlier research.^{3,21} In this study, there are two very sharp IR bands at 1153 and 1084 cm^{-1} which were not observed by Potter and Rossman³ or Luo et al.²¹ These two IR bands were attributed to the deformation of Mn^{3+} -OH bonds.⁴⁸ There were three far IR bands at 512, 477, and 419 cm^{-1} . The first two were taken as characteristic absorption bands of birnessite, and they agree well with the results from Luo et al.²¹

Table 1 shows the EDS data of 25 points of sodium (Na) and manganese (Mn) contents in a birnessite particle. There are only two points having higher Na to Mn molar ratios than 0.06. On the other hand, the Na content in 11 of 25 points is beyond the detectable limit of EDS.

Discussion

Comparison of ODPR Approach with the Conventional OPO and OPP Methods. The ODPR approach is essentially a modification of the OPO method.^{22,23} In the ODPR approach, we can synthesize well-crystallized birnessite at 273 K in 1–4 M NaOH solutions and at high oxygen flow rate with violent agitation.^{45,46} If oxygen can be carefully kept away from the Mn^{2+} solution and pyrochroite suspension in the beginning, reproducible precipitates of birnessite can be synthesized within a short time. Keeping oxygen away from the Mn^{2+} and NaOH solutions used in the synthesis is a key factor in determining whether birnessite or hausmannite is the final product. There are numerous studies on the synthesis of birnessite. Nonetheless,

(47) Giovanoli, R. *Miner. Deposita* **1980**, *14*, 249.

(48) Farmer, V. C. *Miner. Soc. London* **1975**, 154.

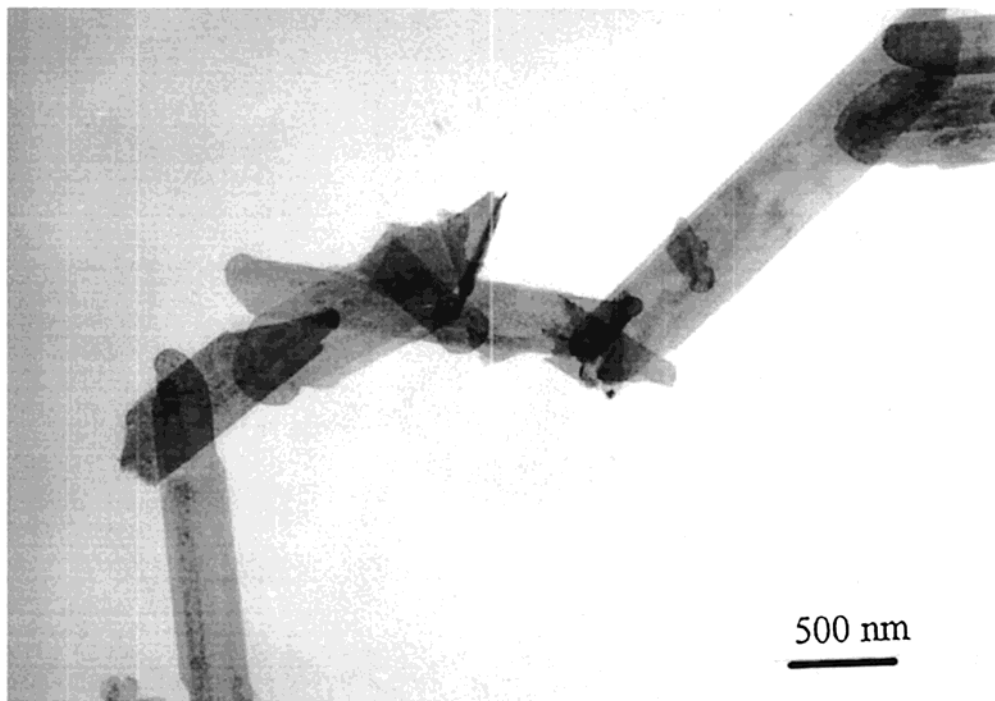


Figure 2. Morphology of birnessite observed by TEM.

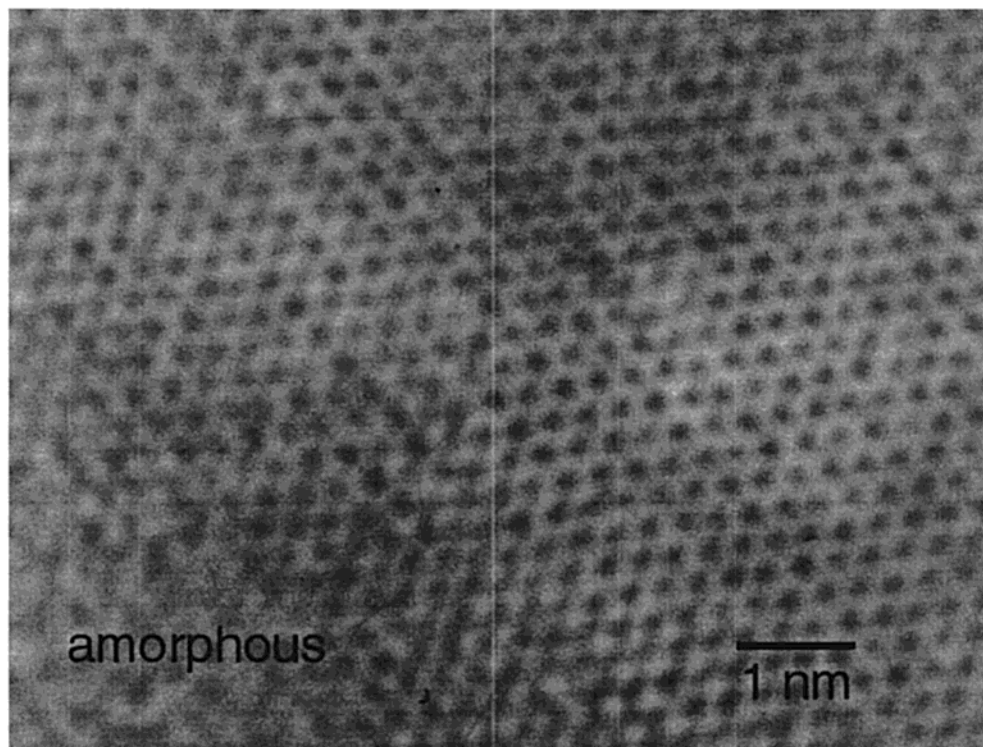


Figure 3. Lattice image of birnessite with an amorphous domain on the lower left corner, observed by HRTEM.

no emphasis has ever been made on the need for oxygen and free Mn^{3+} to be excluded rigorously from the NaOH solutions before they are mixed when preparing pyrochroite. Therefore, hausmannite may exist as impurity, or even worse, hausmannite instead of birnessite can be obtained.

Luo et al.²¹ used permanganate instead of oxygen as an oxidant to transform pyrochroite into birnessite (OPP method). The ODPR approach differs from the OPP method in the following ways.

1. The ODPR approach requires nitrogen gas in the Mn^{2+} and NaOH solutions to exclude free Mn^{3+} in solution before they are mixed to form pyrochroite.

2. The ODPR approach is relatively easier than the OPP method. There are two possible reactions involved in the OPP method, one of the reduction of permanganate by pyrochroite, and the other, the oxidation of pyrochroite by permanganate.

3. Pyrochroite transforms completely into random stacked birnessite within 5 h at 273 K in solutions of

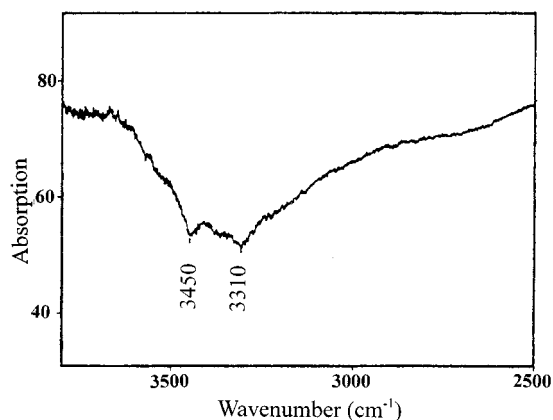


Figure 4. Mid-IR spectrum of birnessite in the range from 3800 to 2500 cm^{-1} .

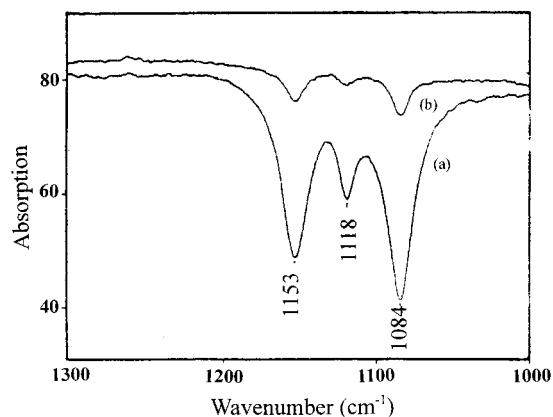


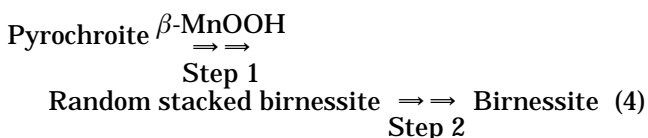
Figure 5. Mid-IR spectrum of (a) birnessite and (b) feitknechtite in the range from 1300 to 1000 cm^{-1} .

NaOH within the range 1–4 M. In contrast, it takes more than 30 days for only 8% conversion to birnessite at a similar temperature by the OPP method.²¹ The initial blue tint suspension is submicron birnessite. The crystallinity of birnessite increases with increasing alkalinity. Aging the 273 K suspension of submicron birnessite at 313 or 373 K for 48 h produces well-crystallized birnessite.

Despite the differences, there are also several similarities between the ODP approach and OPP method. First, the crystallization of birnessite is favored at higher temperature but impeded at 273 K. Second, as the basicity increases, the rate of pyrochroite transforming into birnessite accelerates. Third, feitknechtite (β -MnOOH) is an intermediate phase of pyrochroite which can form birnessite. From our preliminary tests, β -MnOOH becomes unstable with increasing pH and can be further oxidized to form random stacked birnessite even at 273 K.

With the ODP approach, β -MnOOH was completely oxidized within 5 h.

Thus, considering the results of the OPP and ODP methods, the target reaction of the ODP (eq 4) can be re-defined as



Step 1: $\text{Mn}^{2+}\text{-OH}$ is quickly oxidized to $\text{Mn}^{3+}\text{-OH}$ and further oxidized, followed by hydrolysis that forms random stacked birnessite.

Step 2: Random stacked birnessite ages at high temperature (above ambient temperature), and transforms into birnessite.

Vacancies in the Birnessite Structure. The structure of birnessite has been studied since the 1970s. Giovanoli et al.^{22,23} were among the pioneers in this research. According to the electron diffraction and powder XRD patterns, Giovanoli et al.^{22,23} claimed that the structure of birnessite is analogous to that of chalcophanite. Thus, birnessite belongs to the phyllo-manganate family with two characteristic properties. First, one out of seven Mn^{4+} octahedral sites is vacant in every manganese octahedral layer, and second, H_2O , OH^- , Na^+ , and Mn^{2+} can exist between two manganese octahedral layers. They suggested that cations located beneath or above the octahedral vacancies in the inter-layer act to balance charges from these vacancies. In addition, the presence of water and hydroxyl molecules, which coordinate with cations in the interlayers, is to offer hydrogen bonds to stabilize the structure of birnessite. Although Giovanoli et al.^{22,23} provided a detailed description of the structure of birnessite, they fell short of gaining a full picture of the birnessite structure.

Manceau and Combes⁴⁹ showed that the ratio of vacant to occupied octahedra is around 1:6 according to the result of extended X-ray absorption fine structure (EXAFS). Manceau and Combes⁴⁹ also assumed that there are Mn^{3+} octahedra beneath or above the vacant sites. Thereafter, they suggested that the structure of birnessite is not two-dimensional. On the other hand, Stouff and Boulegue⁵⁰ also used EXAFS to study the structure of birnessite. They reported that there are vacancies in the manganese octahedral layers, but did not describe the ratio of empty to occupied octahedrons. Post and Veblen³⁹ studied the birnessite structure using Rietveld refinement of powder XRD data. They reported that the ratio of vacancies to occupied sites is 1:16 if vacancies exist in the structure of birnessite. They also claimed that there are no vacancies at all but only Mn^{3+} occupying the Mn^{4+} positions in the octahedral layers. Post and Veblen³⁹ suspected that vacancies exist in the birnessite structure, but found no support from the work of Manceau et al.^{51,52} Results of the study of Manceau et al.^{51,52} agreed with Giovanoli's proposal^{22,23} that the structure of birnessite is the same as that of chalcophanite. On the other hand, Drits et al.⁵³ reported that Na–birnessite is considered as almost vacancy-free in the manganese octahedral layer. However, when Na–birnessite was treated with acid of pH 2 and 3, H–birnessite was formed containing vacancies in the octahedral layer.⁵³ Furthermore, they argued that the sites of layer vacancies are inhibited from the Mn^{3+} sites in Na–birnessite.

Giovanoli et al.^{22,23} suggested that the structural formula of birnessite is $\text{Na}_4\text{Mn}_{14}\text{O}_{27}\cdot 9\text{H}_2\text{O}$. Thus, the

(49) Manceau, A.; Combes, J. M. *Phys. Chem. Miner.* **1988**, *15*, 285.

(50) Stouff, P.; Boulegue, J. *Am. Miner.* **1988**, *73*, 1162.

(51) Manceau, A.; Gorshov, A. I.; Drits, V. A. *Am. Mineral.* **1992**, *77*, 1133.

(52) Manceau, A.; Gorshkov, A. I.; Drits, V. A. *Am. Mineral.* **1992**, *77*, 1144.

(53) Drits, V. A.; Silvester, E.; Gorshkov, A. I.; Manceau, A. *Am. Mineral.* **1997**, *82*, 946.

molar ratio of Na to Mn in birnessite should be 0.222. The function of Na^+ in birnessite is for balancing the charges when vacancies exist in the octahedral sheets. On the other hand, Drits et al.⁵³ have recently proposed that the ideal structural formula of birnessite is $\text{Na}_{0.333}(\text{Mn}^{4+}_{0.722}\text{Mn}^{3+}_{0.222}\text{Mn}^{2+}_{0.055})\text{O}_2$. Besides these, numerous structural formulas of birnessite have been reported. Nevertheless, the presence of sodium in the birnessite structure has never been doubted. If the structural formula of birnessite proposed by Giovanoli et al.^{22,23} or Drits et al.⁵³ was correct, the molar ratio of Na to Mn should be 0.222 in Giovanoli's model or 0.246 in Drits' case. The Na contents from EDS analysis of birnessite are shown in Table 1. Whether the sites being analyzed were edges of particles or not (Figure 3), the Na content was much lower than that proposed in an ideal formula.^{22,23,51} Moreover, the sodium content of 11 out of 25 points was too low to be detected by EDS and 7 out of 25 points contained only trace amounts of sodium. This result shows that the sodium content is much lower than the amount of sodium needed to balance the charges if octahedral sheets do have vacancies as proposed by Giovanoli et al.^{22,23} and Drits.⁵¹ Our observation does not conflict with the results of HRTEM and supports the argument for the ratio of vacancies as 1:16.³⁹ In general, both the HRTEM observations and sodium contents from EDS indicate that there are no vacancies in the octahedral sheets of birnessite. Concerning the role of sodium, trace amounts of sodium may act to compensate for charge imbalances arising from structural disorder and/or may be adsorbed on the surface of birnessite.

Implications of IR Bands. The average oxidation states (AOS) of Mn-oxide showed that the 1 M NaOH and 4 M NaOH were used to oxidize pyrochroite suspensions. The AOS of birnessite in 1 M NaOH was 3.77 and that in 4 M NaOH was 3.87.⁴⁶ These indicate that the oxidation state of Mn is not four or that some Mn^{3+} occupies the Mn^{4+} sites in the birnessite structure. The IR spectra of birnessite and feitknechtite (β - MnOOH) showed IR bands at 1153 and 1084 cm^{-1} (Figure 5). Farmer⁴⁸ attributed these two IR bands to Mn^{3+} -OH vibration. These two new characteristic bands of IR spectra, 1153 and 1084 cm^{-1} , and the AOS value of birnessite again support the arguments of Post and Veblen.³⁹ Thus, there are Mn^{3+} ions existing in the structure of birnessite. These Mn^{3+} ions may appear in the interlayer and/or in the octahedral layers. As seen

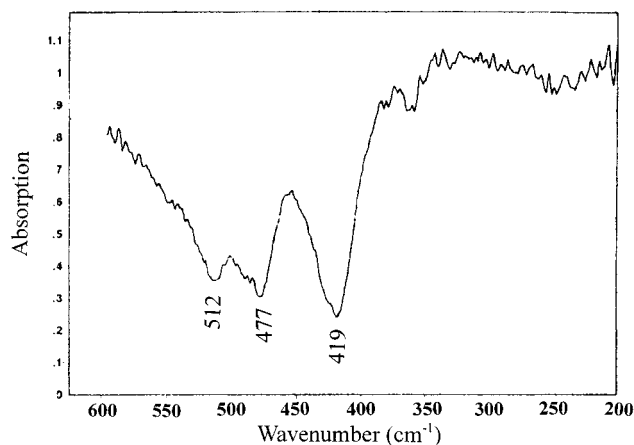


Figure 6. Far-IR spectrum of birnessite between 600 and 200 cm^{-1} .

in the IR spectra of Figures 4–6, the 512- and 477- cm^{-1} bands are characteristic IR bands of birnessite.^{3,21} There are two other groups of IR bands. The first group includes IR bands between 3800 and 2500 cm^{-1} (Figure 4). These are all broad bands; only the 3450- and 3310- cm^{-1} IR bands can be recognized. This suggests that there are water molecules or hydroxyl groups in the interlayers of birnessite. Whether this result agrees or conflicts with the claim of Giovanoli et al.^{22,23} that H_2O , OH^- , Na^+ , and Mn^{2+} exist in the interlayer between two manganese octahedral layers remains unclear. Giovanoli et al.^{22,23} also reported that cations located beneath or above the octahedral vacancies in the interlayer act to balance charges from these vacancies. However, water and hydroxyl groups coordinate with cations in the interlayer. Whether hydrogen bonding serves to stabilize the birnessite structure requires further study.

Conclusions

Well-crystallized birnessite without any impurities can be synthesized between 273 and 373 K within a short time using the ODP approach.

Acknowledgment. This work was financially supported by the National Science Council, Taiwan, ROC, under Projects NSC 87-2811-M002-042, 87-2321-B002-014, and 88-2313-B002-021.

CM010010E